Accepted Manuscript

Numerical modeling of possible lower ionospheric anomalies associated with Nepal earthquake in May, 2015

Suman Chakraborty, Sudipta Sasmal, Tamal Basak, Soujan Ghosh, Sourav Palit, Sandip K. Chakrabarti, Suman Ray Anjan Samanta

Please cite this article as: Chakraborty, S., Sasmal, S., Basak, T., Ghosh, S., Palit, S., Chakrabarti, S.K., Ray, S., A.,Samanta

Numerical modeling of possible lower ionospheric anomalies associated with Nepal earthquake in May, 2015

Suman Chakraborty[a,1,*], Sudipta Sasmal[a], Tamal Basak[a], Soujan Ghosh[a],

Sourav Palit[a], Sandip K. Chakrabarti[b,a], Suman Ray[a] Anjan Samanta[a]

[a]*Indian Centre for Space Physics, 43 Chalantika, Garia Station Road, Kolkata - 700084* [b]*S. N. Bose National Centre for Basic Sciences, JD Block, Sector-III, Salt Lake, Kolkata - 700098*

Abstract

We present perturbations due to seismo-ionospheric coupling processes in propagation characteristics of sub-ionospheric Very Low Frequency (VLF) signals received at Ionospheric & Earthquake Research Centre (IERC) (Lat. $22.50°$ N, Long. $87.48°$ E), India. The study is done during and prior to an earthquake of Richter scale magnitude M=7.3 occurring at a depth of 18 km at southeast of Kodari, Nepal on 12 May 2015 at 12:35:19 IST (07:05:19 UT). The recorded VLF signal of Japanese transmitter JJI at frequency 22.2 kHz (Lat. $32.08°$ N, Long. $130.83°$ E) suffers from strong shifts in sunrise and sunset terminator times towards nighttime starting from three to four days prior to the earthquake. The signal shows a similar variation in terminator times during a major aftershock of magnitude M=6.7 on 16 May, 2015 at 17:04:10 IST (11:34:10 UT). These shifts in terminator times is numerically modeled

[1] Tel: 91-33-2436 6003; Ext. 21

using Long Wavelength Propagation Capability (LWPC) Programme. The unperturbed VLF signal is simulated by using the day and night variation of reflection height (h) and steepness parameter (β) fed in LWPC for the

*Corresponding author

Email addresses: suman.chakrabarty37@gmail.com (Suman Chakraborty), meet2ss25@gmail.com (Sudipta Sasmal), tamalbasak@gmail.com (Tamal Basak), soujanghosh89@gmail.com (Soujan Ghosh), souravspace@gmail.com (Sourav Palit), sandipchakrabarti9@gmail.com (Sandip K. Chakrabarti), sumanray07@gmail.com (Suman Ray)

entire path. The perturbed signal is obtained by additional variation of these parameters inside the earthquake preparation zone. It is found that the shift of the terminator time towards nighttime happens only when the reflection height is increased. We also calculate electron density profile by using the Wait's exponential formula for specified location over the propagation path.

Keywords: Earthquake; Lower ionospheric anomalies; Solar terminator; VLF.

1. Introduction

It is well established since the last five decades (Gokhberg et al., 1982; Garmash et al., 1989; Gokhberg et al., 1989; Hayakawa et al., 1994; Baba et al., 1996; Hayakawa et al., 1996; Rodger et al., 1996; Molchanov and Hayakawa, 1998; Molchanov et al., 1998; Hayakawa et al., 1999; Clilverd et al., 1999 ; Liu et al., 1999; Kang et al., 2001; Karpova et al., 2002; Miyaki et al., 2002 ; Rozhnoi et al., 2004; Pulinets et al., 2004; Horie et al., 2007a; Horie et al., 2007b; Ouzonov et al., 2007; Rozhnoi et al., 2007a,b; Nemec et al., 2009 ; Korepanov et al., 2009; Molchanov et al., 2009; Muto et al., 2009; Blaunstein et al., 2009; Hayakawa et al., 2010; Ouzonov et al., 2011; Pulinets et al., 2011) that the pre- and post-seismic activities can be strongly correlated with lower ionospheric perturbations. A variety of physical mechanisms were reported for the emission of electromagnetic signals associated with possible earthquake precursors including electro-kinetic phenomena, radioactive emission,

thermal anomalies, Piezo-electric processes, exo-electron etc. According to Lithosphere Atmosphere Ionosphere Coupling (LAIC) mechanism, within the earthquake preparation zone (Dobrovolsky et al., 1979) the pre-seismic process starts much prior to the main earthquake shock and the coupling mechanism can happen through acoustic, chemical and electromagnetic channels. The electromagnetic anomalies can extend from Ultra Low Frequency (ULF) to Very Low Frequency (VLF) range. The seismo-electrodynamics can result in the emission of electromagnetic wave in the form of ULF or it can be a strong perturbation in propagated VLF signals through earthionosphere waveguide. The earthquake preparation mechanism can directly or indirectly perturb the localized ionospheric plasma properties. The excess ionization due to radioactive emission prior to seismic events can generate electric field which increases particle acceleration and the plasma instability. In the context of lower ionospheric layer (D-layer) the charge density profile and the effective reflection height for propagated radio wave thus can be highly perturbed during and before the seismic events. The characteristics of propagated VLF signal through the earth-ionosphere waveguide (EIWG) can thus suffer from anomalies in their amplitude and phase due to this perturbation.

The ionospheric anomalies in radio signal propagated through the EIWG due to seismo-electrodynamics has a wide range of parameters which vary with height. It starts from the unusual day and nighttime amplitude and phase modulation of VLF wave due to change in the modal interference by the change in critical frequency in F2 layer (Pulinets et al., 2002). In the VLF range, vast research has been carried out to examine the precursory phenomena associated with the signal propagation characteristics. It has been observed that the signal amplitude and phase suffer specific perturbation due to earthquakes and which is unusual and has no connection with other solar or extra-terrestrial ionization. One of the well-known methodologies is the sunrise/sunset terminator time shift of the amplitude/phase of the sub-ionospheric VLF signal. The SRT (sunrise terminator time) and SST (sunset terminator time) are the minima in the signal amplitude when the D-layer is almost generated in the morning due to solar flux and it starts to disappear in the evening time respectively towards nighttime. It has been first discovered by Hawakaya et al. (Hayakawa et al.,1996) after the historic Kobe earthquake that the SRT and SST were shifted subsequently before the earthquake. Hayakawa et al. (1996) shows a similar outcome due to many earthquakes. A

3

substantial statistical study has been done (Chakrabarti et al., 2005, 2007, 2010; Ray et al., 2010, 2011, 2012, 2013; Sasmal et al., 2010 , 2014, 2016) which shows that the maximum shift occurs up to 0 to 4 days before a major earthquake. For some particular earthquakes and propagation paths, the shift becomes maximum on the day of the quake. The amount of shift strongly depends on the propagation path. Apart from the terminator shift method, other VLF perturbations have been also found in the signal. These are unusual enhancement of D-layer Preparation Time (DLPT) and D-Layer Disappearance Time (DLDT) before the earthquake (Chakrabarti et al., 2007, 2010; Sasmal et al., 2010), unusual nighttime fluctuations (Both enhancement and decrease) in the signal amplitude (Ray et al., 2011, 2012) , unusual presence of gravity wave in the night time signal etc. In all the above methodologies, the signal suffers maximum perturbation from 0 to 4 days prior to the earthquake (Chakrabarti et al., 2005, 2007, 2010; Ray et al., 2010, 2011, 2012, 2013; Sasmal et al., 2010, 2014, 2016).

The true physical mechanism of the LAIC could be highly complicated due to its anisotropic and multi-parametric nature (Pulinets et al, 2011; Molchanov, 2009). Numerical modeling of D-layer propagation characteristics is also challenging due to the dynamic nature of chemical properties of the layer. From our experience of studying perturbations for a large number of earthquakes, it appears that the terminator time variation during an earthquake strongly   depends on the modal interference and the mode conversion as propagating mode are affected due to change in the electrical conductivity of both ground and ionosphere (Clilverd et al., 1999). Numerical reproduction of terminator time shifts has been reported for a short path from Omega, Japan to Inubo (~ 1100 km) by Hayakawa et al. (1996a, b) and Molchanov et al. (1998). They found a lowering of the VLF reflection height of day and night assuming the enhancement of charge density due to the earthquake. Later a hybrid modefinder model has been used by Rodger et al. (1999), where the ionospheric reflection parameters and the ground parameters were time dependent and the study was executed for both homogeneous and inhomogeneous waveguide conditions. The modal interference was calculated for all the conditions and the model was coupled with Long Wavelength Propagation Capability (LWPC) and Wait's exponential formula to represent the terminator shift.

In this paper, we present a possible physical mechanism of the shift in terminator times for a relatively large propagation path. Significant amount

4

of terminator time shift was observed during the earthquake in Nepal in 2015. We try to reproduce the shift by varying the the reflection height (h')and steepness parameter (β) of the ionosphere. The JJI-IERC propagation path ($\sim$ 4355 km) is longer than those used in previous attempts. As the transmitter is located far east from the receiving location, there is a delay of sunrise and sunset of around 3 hours. Thus, during sunrise and sunset the propagation path is sometimes in (i) fully dark, (ii) fully illuminated and (iii) partly illuminated condition. Under non-seismic condition, we use justifiable values of h and β for the entire path in our modeling to replicate the realistic propagation condition. Secondly, to investigate the effects due to earthquakes on the signal propagation, we vary the parameter values within the Earthquake Preparation Zone (EPZ) (Dobrovolsky, et al., 1979) keeping their values intact outside of the EPZ. We use LWPC programme (Ferguson, 1990) and Wait's exponential formula to interpret the terminator shift process which satisfies our observation.

2. Observation & Analysis

We study VLF signal amplitude variation for the JJI transmitter (Lat. 32.08 ˚ N, Long. 130.83 ˚ E) of frequency 22.2 kHz received at the Ionospheric & Earthquake Research Centre (Lat. 22.50 ˚ N, Long. 87.48 ˚ E). The great circle distance of the propagation path is $\sim$ 4355 km. The signal has been received with an electric field antenna coupled with SoftPAL (Software Amplitude Phase Logger) recording device and software. A major earthquake (Lat. 27.7 ˚ N, Long. 86.0 ˚ E) occurred on 12 May 2015 at 12:35:19 local time (07:05:19 UT) having the Richter scale magnitude of M=7.3 (*Eq*1) and depth 18 km at southeast of Kodari, Nepal. There was a second quake of magnitude M=6.7 (*Eq*2) and depth of 10 km on 16 May (Lat. 27.5 ˚ N, Long. 86.0 ˚ E) at 17:04:10 local time (11:34:10 UT). Figure 1 shows the position of Japanese transmitter JJI (marked with blue triangle), receiving location IERC (marked with black circle) and the wave path between them. The positions of the epicenters of two earthquakes are marked by the red filled circles. The Earthquake Preparation Zones (EPZ) are marked with the grey circles. The radius of the EPZs for *Eq*1 and *Eq*2 are 1377 km and 760 km respectively.

Figure 2 shows the diurnal variation of VLF signal amplitude as a function of time in minutes for the day of 9th May, 2015. It has been observed that at

5

around 05:00:00 local time (LT) the signal suffers from a massive fall in gain and again reaches to normal value at around 14:00:00 LT. We observed this phenomenon on signal amplitude every day during our observation period from 9th to 17th May, 2015. Clearly this is not the actual transmitted VLF signal and may be due to maintenance or other problem at the transmitter end. Fortunately, the duration of the drop of signal amplitude is quite far away from both the sunrise and sunset transmitter times. Therefore, we can easily use the data during sunrise and sunset for analysis.

We monitor the signal amplitude continuously up to 17th May, 2015 and
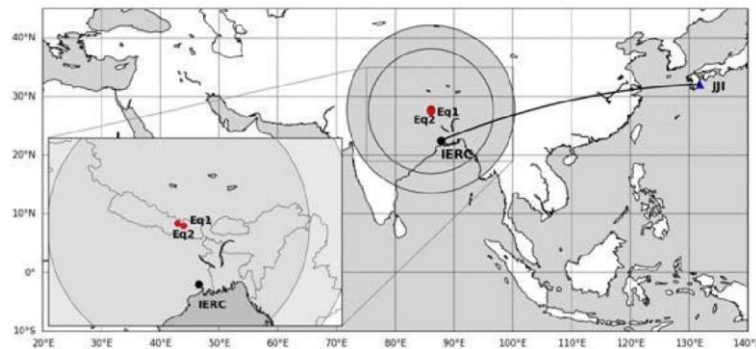

Figure 1: The locations of the transmitter (blue triangle), the receiver (black circle) and the propagation path between them. The earthquake epicenters are marked by red circles and the earthquake preparation zones are the grey shaded circles. The locations of the earthquake epicenters are presented in a magnified way in the inset.

observe significant shifts in both SRT and SST towards nighttime. To eliminate the case of the signal drop on daily basis, we select our data around terminator times and scrutinize variations of SRT and SST during the two earthquakes. Figure 3 presents the variation of SRT as a function of time in minutes from 09/05/2015 to 17/05/2015. The signal amplitudes are stacked with a shift by 10 dB each to check the day to day variation of SRT. The SRTs are indicated by arrows. The normal value before and after the quakes is around 03:56:00 LT. From the Figure, it is clear that the SRT starts to shift towards nighttime

6

from 10th May and the shift is maximum on 11 th May, which is 1 day before the quake. On 12th May, the major shock occurred. After that, there were several aftershocks with small to moderate magnitudes (3 - 5). After 15th of May, the terminator again shifted towards nighttime and reached almost the same position as before the previous earthquake. On 16th May, another strong earthquake occurred with a magnitude of 6.7. On 16th May, the terminator again started to move towards its normal value and on 17th May, it became almost normal as on 9th May. It is clear from the Figure that the movement of SRT towards nighttime is related to the two earthquakes and the anomalous movement of SRT towards nighttime

occurred before the seismic events. In Figure 4, we present the similar variation of SST from 09/05/2015 to 17/05/2015. The normal value of SST
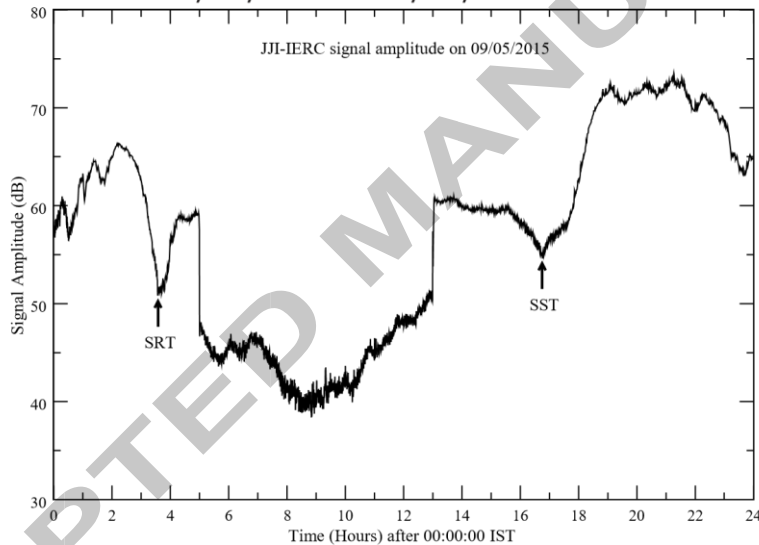

Figure 2: Diurnal variation of VLF signal amplitude as a function of time (in hours) as received at IERC along the path JJI-IERC for 9 May, 2015. The SRT and SST are the sunrise and sunset terminator time respectively.

before the quake is around 16:30:00 LT. In a similar way, the SST starts to shift towards nighttime from 10th May and the shift is maximum on 11 th May, which is 1 day before the quake. On 13th of May, it came closer to the normal value but again started to move towards nighttime from 14th. For SST, the shift is maximum 2 days prior to the earthquake of 16th May. In comparison to sunrise, there are some sorts of residual anomaly after the two earthquakes and the signal took one more day to become normal.

7

In Figure 5, we compare the variations of SRT (top panel), SST (middle panel) and VLF daylength (bottom panel) obtained from the difference of SST and SRT as a function of the day around the earthquakes. The SRT is minimum, i.e., maximum shift towards nighttime is for 11th and 15th May, both are 1 day prior to the shocks. For SST, the variation differs slightly from the sunrise. For the first quake, SST is maximum (maximum shift towards nighttime) on 11th May and for the second quake it is maxima on 14th May. Thus for the first quake, the value is maximum just 1 day before the event while for the second quake, it is maximum 2 days prior to the event.
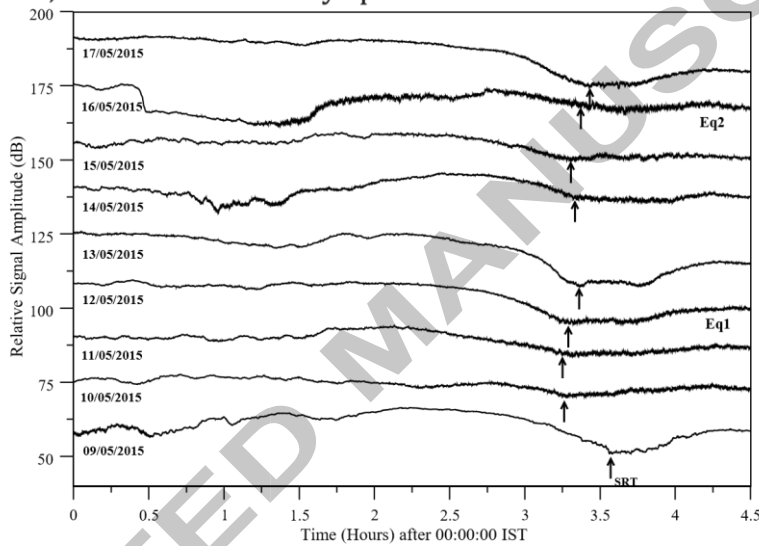

Figure 3: Daily variation of sunrise terminator time (SRT) as a function of time in minutes from 09/05/2015 to 17/05/2015. The signal amplitudes are stacked with a shift by 10 dB each. The SRTs are indicated by arrows. The earthquakes occurred on 12 and 16 May, 2015. For both the earthquakes, the shift is maximum 1 day before the quakes.

3. Numerical Simulation

The propagation path we chose for our study (JJI-IERC) is special in the sense of its significant longitudinal spread between the transmitter and receiver. As a result, it experiences a transverse movement of both sunrise and sunset terminators over it. Hence there is inhomogeneity of solar illumination over the path during both the local sunrise and sunset times. So our primary aim was to follow the true trend of movement of the day-night terminator over the path instead of considering homogeneous illumination/darkness. For this, we

8

first calculate the speed of terminator (v) at our location from the well-known formula

$$v = \frac{2\pi R_{equator} cos(latitude)}{24hr}. \quad (1)$$

Here by substituting the value of latitude as 29° which is the latitude of the midpoint of the propagation path we obtained the value of v as 407 m/sec. This indicates that it will cover almost 25 km distance in 1 minute. In Figure
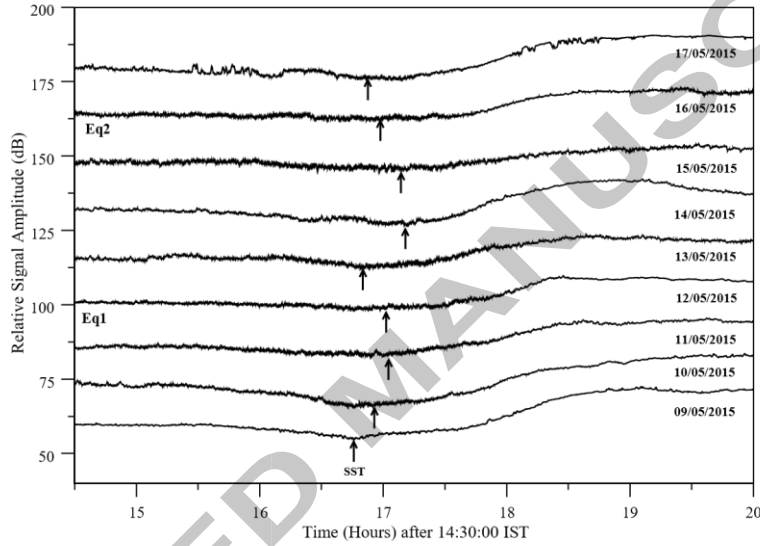

Figure 4: Daily variation of sunset terminator time (SST) as a function of time in minutes from 09/05/2015 to 17/05/2015. The signal amplitudes are stacked with a shift by 10 dB each. The SSTs are indicated by arrows. The earthquakes occurred on 12 and 16 May, 2015. For the 12 May quake the shift is maximum before 1 day whereas for the 16 May quake, the shift is maximum 2 days before the quake.

6, we present the position of the terminator shadow when the transmitter is just illuminated/dark, at the time of SRT/SST and when the receiver is just dark/illuminated respectively. The top three panels are for sunrise and the bottom three panels are for sunset respectively. The other positions of the shadow lie within these above-mentioned conditions.

This inhomogeneous nature of the solar illumination over the propagation path has been incorporated into the RANGE subprogram of LWPC code by dividing the whole path into several segments depending upon the terminator

9

position. In the LWPC code the ionosphere has been defined by the so-called Wait's exponential profiles (Wait et al., 1964; Cummer et al., 1998 ; Clilverd et al., 1999) where the sharpness parameter β and VLF reflection height h control the electron density profile at the D-region. We have taken same β and h values for either of the two regions (illuminated or dark) and considered a sharp change in their values across the shadow boundary. In this way, we obtained the set of parameter values defining signal propagation under normal (non-seismic) scenario.
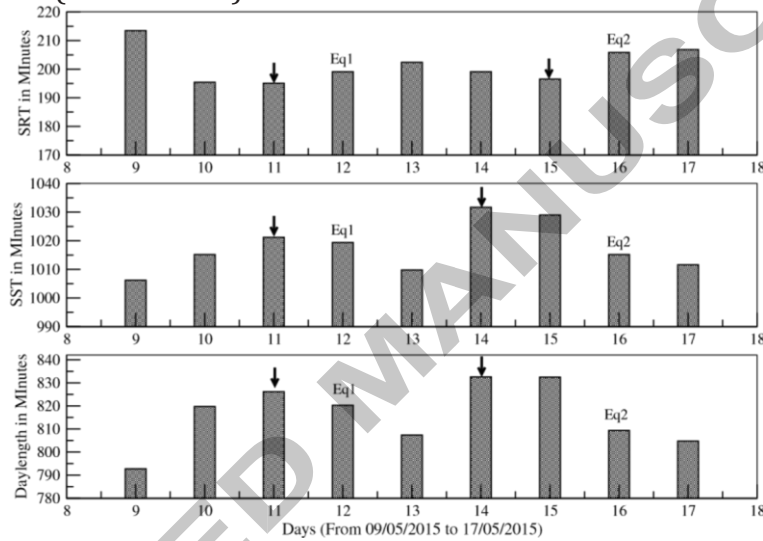

Figure 5: Variation of SRT (top panel), SST (middle panel) and VLF daylength (bottom panel), which is the difference of SST and SRT as a function of day around the earthquakes. For 11th and 15th May, 2015 the shift is maximum 1 day prior to the shocks. For SST, for the first quake, SST is maximum 1 day before the event while for the second quake, it is maximum 2 days prior to the event.

It is clear from Figure 1 that the EPZ covers only around $1/3^{rd}$ of the propagation path from the receiving end. It is expected that the perturbation in sub-ionospheric propagation of VLF signal due to earthquakes would be confined mostly within this part of the path. So, in our second stage we incorporated additional changes of the ionospheric parameters only within this portion. Outside of EPZ, the parameter values were taken same as under normal (non-seismic) condition. We proceeded by both lowering and raising the parameter values within the range ±3 km for h and ±0.03 km^{-1} for β to check under which condition, the simulation results corroborate the

10

observation. The parameter values taken in our study are given in Table 1. The values corresponding to 'Normal' are for the whole propagation path under non-seismic condition and that portion of the path outside the EPZ 'Lowering' and 'Raising' are for that portion of the propagation path that is within the EPZ.

Figure 6: The illumination/darkness condition at transmitter, receiver and its midpoint during the sunrise and sunset on May 9, 2015. The upper panels shows the terminator shadow when (left) the transmitter is just illuminated, (middle) at sunrise terminator time at receiving location and (right) when the receiver is just illuminated. The lower panel shows a similar condition during the sunset when (left) the transmitter is just facing the darkness, (middle) at the sunset terminator time at receiving location and (right) when the receiver is just facing the darkness.
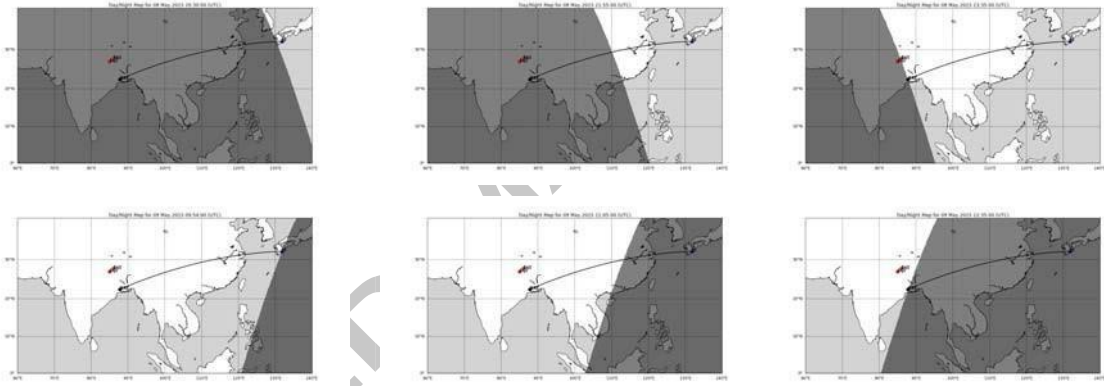
under an anomalous (seismic) condition. The same corresponding to
Next to calculate electron density the well-known Wait's formula was used (Wait, 1962 a,b; Thomson, 1993; Grubor, 2008)

$$N_e(h, h', \beta) = 1.43 \times 10^{13} exp(-0.15h') \; exp[(\beta - 0.15)(h - h')] \quad , (2)$$

where N_e is in m^{-3}.

Here, by substituting the values of β and h both for non-seismic and seismic conditions, we obtain the height profile of electron density at different times and positions over the propagation path.

11

4. Results and Interpretations

In Figure 7, we present the VLF signal amplitude as a function of time as obtained from LWPC simulations starting from 2 A.M. to 5 A.M. IST. The black curve indicates the signal under non-seismic condition, and the green curve and the red curve indicate the signal as obtained by respectively lowering and raising the parameters β and h within the EPZ (parameter values are in Table 1). The dotted vertical lines indicate corresponding SRTs. From the figure, we clearly see that by raising the ionosphere within the EPZ, the Table 1: D region ionospheric parameter values used in numerical modelling

Condition	Illuminated Region $[h'(\text{km})/\beta(\text{km}^{-1})]$	Dark Region $[h'(\text{km})/\beta(\text{km}^{-1})]$
Non-seismic	75.0/0.35	85.0/0.55
Seismic (i) Lowering	72.0/0.32	83.0/0.53
(ii) Raising	78.0/0.38	87.0/0.57

SRT shifts towards nighttime by 10 minutes whereas the shift in SRT from observation is ~ 17 minutes.

In Figure 8, we plot the VLF signal amplitude during the sunset starting from 3 P.M. to 6 P.M. IST as obtained from LWPC simulations. Here also the black curve indicates the signal under non-seismic condition, and the green curve and the red curve indicate the signal corresponding to seismic condition obtained by respectively lowering and raising the ionospheric parameters β and h within the EPZ (parameter values are in Table 1). The vertical dotted lines indicate the corresponding SSTs. From this figure too, we see that by raising the ionosphere within the EPZ, the SST shifts towards nighttime by 15 minutes which exactly agrees our observation.

We therefore see that by raising the ionosphere within the EPZ, the daylength increases by almost 25 minutes. From our observation, we saw that the maximum shift of both the terminator times was on May 11, 2015 that resulted in daylength increase of almost 32 minutes.

In Figure 9 we present the height profile of electron density in m^{-3} in logarithmic scale as a function of ionospheric height in km as obtained from our simulation. The top panels are for the transmitting location (T), the middle panels are for the mid-point of the propagation path (M) and the bottom panels are for the receiving location (R). The figures on the left are for SRT and those on the right are for SST. The black curve indicates the electron density profile under non-seismic condition, and the green and red curves indicate that obtained by respective lowering and raising the ionosphere within the EPZ. From the figure, we see that raising the ionosphere within the EPZ implies a decrease in overall electron density.
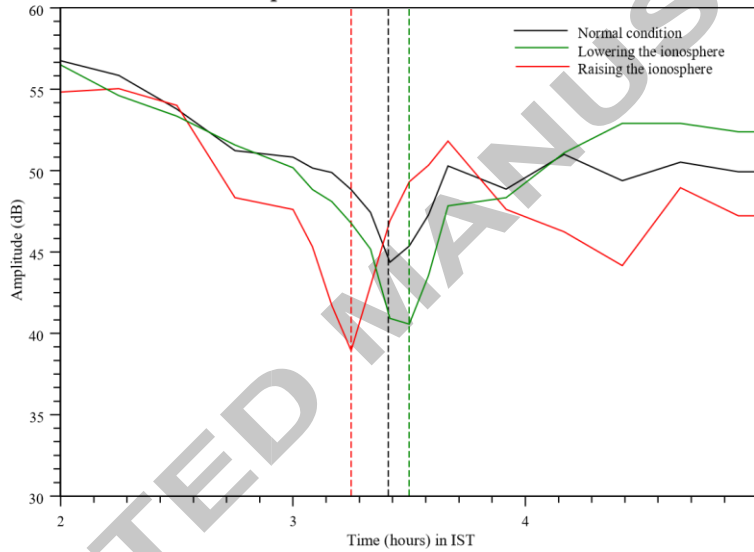

Figure 7: Simulated VLF amplitude under non-seismic and seismic conditions during sunrise. The black curve represents the non-seismic condition whereas the green and red curves represent seismic condition obtained by lowering and raising the β and h parameters within the EPZ in LWPC within the range ±3km for h and ±0.03km^{-1} for β. The vertical lines represent the corresponding sunrise terminator times (SRTs).

In order to eliminate the possibility that the effects of solar geomagnetism (if any) could have influenced our observational results we study the behavior of the solar geomagnetic Kp index during our observation period. Figure 10 shows the variation of Kp index from May 5 to 20, 2015. The value of Kp was always less than 5 which can be treated as geomagnetically quiet. Most of the values of Kp lies below 3.5 except on May 13 where it goes to ~ 4.9. However, it is on the day after the main shock. So, the seismo-ionospheric effects may

be safely assumed not to have been contaminated by any solar geomagnetic activities.

5. Conclusion

In this paper, we study the nature of anomaly in VLF signal amplitude before and during the Nepal earthquake in May, 2015. The path we chose for
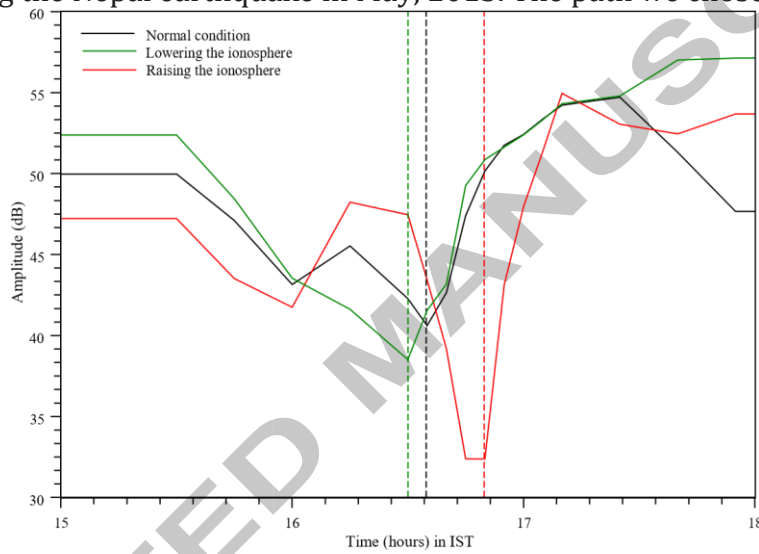

Figure 8: Simulated VLF amplitude for normal and perturbed days during sunset. The black curve represents the non-seismic condition whereas the green and red curves represent seismic condition obtained by lowering and raising the β and h parameters within the EPZ in LWPC within the range ±3km for h' and $\pm 0.03\text{km}^{-1}$ for β. The vertical lines represent the corresponding sunset terminator times (SSTs).

our study was JJI-IERC. This particular propagation path has a special feature that, being primarily along the east-west, it has a very high longitudinal variation. As a result, the solar zenith angle over the path was highly variable. For instance, when the transmitter, namely JJI was in sunlit condition, the receiver, namely IERC was experiencing night condition. So our primary focus was to vary the solar illumination over the entire path following the true trend of movement of solar terminator and generate the 'normal' diurnal signal. We did so by calculating the speed of solar terminator at our location and then by incorporating this into the RANGE subprogram of LWPC code. We assume that the ionospheric parameters β and h for either of the two regions (illumination

14

or darkness) remain separately fixed and the sharp change in their values take place only across the shadow boundary. This assumption was well justified since the path of study was very long ($\sim$ 4355 km) as compared to the few hundreds of kms of twilight region around the terminator boundary. Furthermore, since the LWPC is a numerical simulation code, it calculates the signal characteristics by estimating the contributions from different modes on each propagation path segment. Each
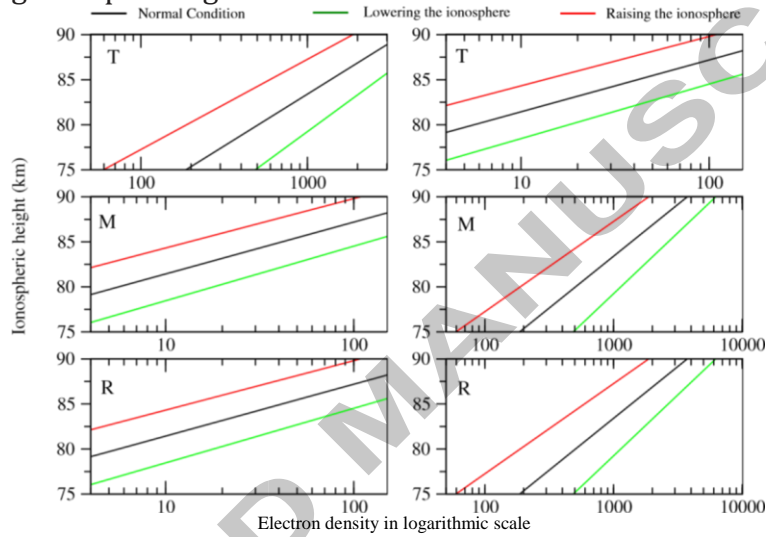

Figure 9: Variation of electron density in m^{-3} in logarithmic scale as a function of ionospheric height in km. The top panel is for the transmitting location, middle for mid-point of propagation path and bottom panel for receiving location. It is clear that the electron density decreases before the earthquake.

of those segments is typically hundreds of kilometers long. So the sharp terminator approximation instead of true twilight ionosphere profile would not affect much. After we reproduced the normal signal at the terminators, we then tried to study the propagation of signal under seismic condition. In this context, we should mention the famous Dobrovolsky formula which defines a region around the earthquake epicenter where the effects of a particular earthquake can be identified. This zone is called the earthquake preparation zone (EPZ) [Dobrovolsky et al., 1979]. For earthquakes of magnitude M = 7.3 and M = 6.7, this EPZ would be 1377 km and 760 km respectively as prescribed by Dobrovolsky. So, in our case only about 1/3rd of the propagation path was within the EPZ. We incorporated this effect into our simulation by raising and lowering the parameters β and h only for that portion of the

15

propagation path that lied within the EPZ. For the rest of the propagation path, we kept the values as it was under normal condition. With this proposition and modifications in our model, we found that raising of these parameters within the EPZ reproduced the shifts of terminators, both SRT and SST as observed. We obtained an increase of daylength by almost 25 minutes whereas the same as observed was 32 minutes on May 11.
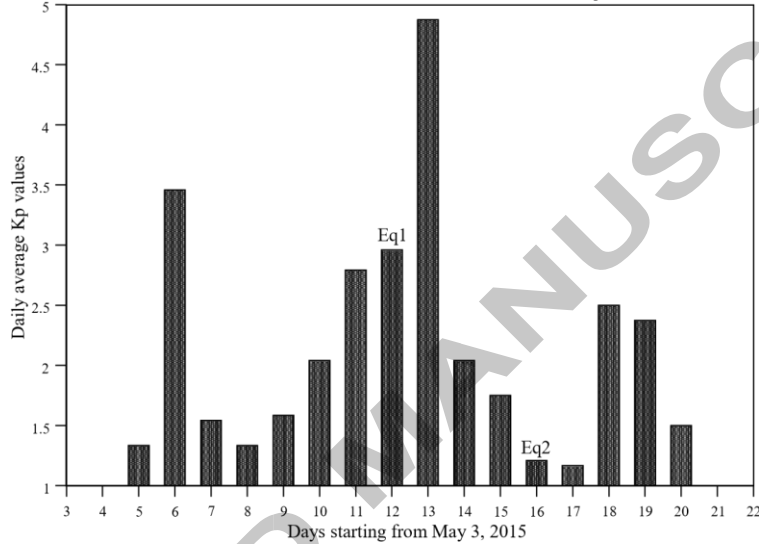

Figure 10: Variation of solar geomagnetic *Kp* index from May 5 to 20, 2015. The value of k_p is always less than 5 during the entire observation period which implies quiet geomagnetic condition.

From our simulation we also found that the electron density decreases before the earthquake. Using several satellite and ground-based measurements, Trigunait et al. (2004) also observed a similar decrease in overall ionospheric electron content before the Bhuj earthquake. Hence we can conclude that from our model we could achieve at least the order and nature of terminator shift, both SRT and SST prior to an earthquake. Obviously, there are some mismatches which arise from our consideration of sharp change in the parameter values across the EPZ boundary which is not a true realistic scenario but still a justifiable approximation to make that is also evident from the results obtained. Future detailed study and improvement of the model may lead to more accuracy in the results.

16

Baba, K., and Hayakawa, M., 1996, Computational results of the effect of localized ionospheric perturbations on subionospheric VLF propagation, J. Geophys. Res., 101, pp.10985–10993.

Budden, K.G., 1961, The Wave-Guide Mode Theory of Wave Propagation, Logos Press, Prentice-Hall, London.

Blaunstein, N. and Hayakawa, M., 2009, Short-term ionospheric precursors of earthquakes using vertical and oblique ionosondes, Phys. Chem. Earth, Parts A/B/C, Electromagnetic Phenomena Associated with Earthquakes and Volcanoes, edited by: M. Hayakawa, J.Y. Liu, K. Hattori and L. Telesca, 34(6–7), pp.496–507.

Chakrabarti S.K., Saha, M., Khan, R., Mandal, S., Acharyya, K. and Saha, R., 2005, Possible detection of ionospheric disturbances during SumatraAndaman Islands earthquakes in December, Indian J. Radio and Space Phys., 34, pp.314–317.

Chakrabarti, S., Sasmal, S., Saha, M., Khan, M., Bhowmik, D. and Chakrabarti, S.K., 2007, Unusual behavior of D-region ionization time at 18.2 kHz during seismically active days, Indian J. Phys., 81, pp.531–538.

Chakrabarti, S.K., Sasmal, S. and Chakrabarti, S., 2010, Ionospheric anomaly due to seismic activities-II: Possible evidence from D-layer preparation and disappearance times, Nat. Haz. Earth Syst. Sci., 10, pp.1751– 1757.

Clilverd, M.A., Rodger, C.J. and Thomson, N.R., 1999, Investigating seismoionospheric effects on a long subionospheric path, J. Geophys. Res., 104(A12), pp.28171–28179.

Cummer, S.A., Inan, U.S. and Bell, T.F., 1998, Ionospheric D region remote sensing using VLF radio atmospherics, Radio Sci., 33, pp.1781–1792.

Deshpande, S.D. and Mitra, A.P., 1972, Ionospheric effects of solar flares-IV. Electron density profiles deduced from measurements of SCNA's and VLF phase and amplitude, J. Atmos. Terr. Phys., 34, pp.255–266.

17

Dobrovolsky, I.R., Zubkov, S.I. and Myachkin, V.I., 1979, Estimation of the size of earthquake preparation zones, Pageoph., 117, pp.1025–1044.

Ferguson, J.A., and Snyder, F. P., 1990, Computer programs for assessment of long wavelength radio communications, Version 1.0: Full FORTRAN code users guide, TD 1773, Nav. Ocean Syst. Cent., San Diego, California.

Garmash, S.V., Linkov, E.M., Petrova, L.N. and Shved, G.M., 1989, Generation of atmospheric oscillations by seismic-gravity oscillations of the Earth, Izvestiya, Atmos. Oceanic Phys., 25, pp.952–959.

Gokhberg, M.B., Morgounov, V.A., Yoshino, T. and Tomizawa, I., 1982 , Experimental measurement of electromagnetic emissions possibly related to earthquakes in Japan, J. Geophys. Res., 87(B9), pp.7824–7828.

Gokhberg, M.B., Gufeld, I.L., Rozhnoy, A.A., Marenko, V.F., Yampolsky, V.S. and Ponomarev, E.A., 1989, Study of seismic influence on the ionosphere by super long-wave probing of the Earth ionosphere wave-guide, Phys. Ear. Planet. Inter., 57, pp.64–67.

Gufeld, I., Gusev, G. and Pokhotelov, O., 1994, Is the prediction of earthquake dates possible by the VLF radio wave method in Electromagnetic Phenomena Related to Earthquake Prediction, edited by: M. Hayakawa and Y. Fujinawa, Terra. Sci. Pub. Co., Tokyo, pp.381–389.

Hayakawa, M., and Fujinawa, Y., 1994, Electromagnetic Phenomena Related to Earthquake Prediction, Terra Sci. Pub. Co., Tokyo, pp.67–71.

Hayakawa, M., and Sato, H., 1994, Ionospheric perturbations associated with earthquakes as detected by subionospheric VLF propagation in Electromagnetic Phenomena Related to Earthquake Prediction, edited by: M. Hayakawa and Y.Fujinawa, Terra Sci. Pub. Co., Tokyo, pp.391–397.

Hayakawa, M., Molchanov, O.A., Ondoh, T. and Kawai, E., 1996a, Anomalies in the sub-ionospheric VLF signals for the 1995 Hyogo-ken Nanbu earthquake, J. Phys. Earth, 44, pp.413–418.

Hayakawa, M., Molchanov, O. A., Ondoh, T., and Kawai, E., 1996b, The precursory signature effect of the Kobe earthquake on VLF subionospheric signals, J. Comm. Res. Lab., Tokyo, 43, pp.169–180.

Hayakawa, M., 1999, Atmospheric and Ionospheric Electromagnetic Phenomena Associated with Earthquakes, Terra Sci. Pub. Co., Tokyo, 996 pp.

Hayakawa, M. and Molchanov, O.A., 2002, Seismo Electromagnetics: Lithosphere-Atmosphere-Ionosphere Coupling, edited by: M. Hayakawa, Terrapub, Tokyo, pp.477–482.

Hayakawa, M., Ohta, K., Nickolaenko, A.P. and Ando, Y., 2005, Anomalous effect in Schumann resonance phenomena observed in Japan, possibly associated with the Chi-chi earthquake in Taiwan, Ann. Geophys., 23 , pp.1335–1346.

Hayakawa, M., Kasahara, Y., Nakamura, T., Muto, F., Horie, T., Maekawa, S., Hobara, Y., Rozhnoi, A., Solovieva, M., and Molchanov, O.A., 2010 , A statistical study on the correlation between lower ionospheric perturbations as seen by subionospheric VLF/LF propagation and earthquakes, J. Geophys. Res., 115, A09305, doi:10.1029/2009JA015143.

Hines, C.O., 1974, Tidal oscillations, shorter period gravity waves and shear waves, The Upper Atmosphere in Motion, Geophys. Monogr. Ser., American Geophysical Union, Washington, D. C., 18, doi: 10.1029 /GM018p0096, pp.96–109.

Horie, T., Maekawa, S., Yamauchi, T. and Hayakawa, M., 2007a, A possible effect of ionospheric perturbations associated with the Sumatra earthquake, as revealed from subionospheric very-low-frequency (VLF) propagation (NWC-Japan), Int. J. Remote Sens., 28, pp.3133–3139.

Horie, T., Yamauchi, T., Yoshida, M. and Hayakawa, M., 2007b, The wave like structures of ionospheric perturbation associated with Sumatra earthquake of 26 December 2004, as revealed from VLF observation in Japan of NWC signals, J. Atmos. Sol.-Terr. Phys., 69, pp.1021–1028.

Kang, C. and Liu, D., 2001, The applicability of satellite remote sensing in monitoring earthquake, Science of Surveying and Mapping, 26, pp.46–48.

Karpova, N.V., Petrova, L.N., and Shved, G.M., 2002, Statistical study of seismic and ground pressure oscillations with steady frequencies in the 0.7–5 h period range, Ann. Geophys., 20, pp.823–833.

19

Korepanov, V., Hayakawa, M., Yampolski, Y., and Lizunov, G., 2009, AGW as a seismo-ionospheric responsible agent, Phys. Chem. Earth, 34(6-7) , pp.485–495.

Liebmann, B. and Smith, C.A., 1996, Description of a Complete (Interpolated) Outgoing Longwave Radiation Dataset, Bull. Am. Meteorol. Soc, 77 (6), U. S. A., pp.1275–1277.

Liu, D., Peng, K., Liu, W., Li, L. and Hou, Z., 1999, Thermal omens before earthquake, Acta Seimol. Sin, 12, pp.710–715.

Liu, D., 2000, Anomalies analysis on satellite remote sensing OLR before Jiji earthquake of Taiwan Province, Geo-Information Science, 2(1), pp.33–36.

Miyaki, K., Hayakawa, M. and Molchanov, O.A., 2002, The role of gravity waves in the lithosphere-ionosphere coupling, as revealed from the subionospheric LF propagation data in Seismo-Electromagnetics (LithosphereAtmosphere-Ionosphere Coupling), edited by: M. Hayakawa and O. Molchanov, Terrapub, Tokyo, pp.229–232.

Molchanov, O.A. and Hayakawa, M., 1998, Subionospheric VLF signal perturbations possibly related to earthquakes, J. Geophys. Res., 103 , pp.17489–17504.

Molchanov, O.A., Hayakawa, M., Ondoh, T., and Kawai, E., 1998, Precursory effects in the subionospheric VLF signals for the Kobe earthquake, Phys. Earth Planet Inter., 105, pp.239–248.

Molchanov, O.A., 2009, Lithosphere-Atmosphere-Ionosphere Coupling due to Seismicity, Electromagnetic Phenomena Associated with Earthquakes, edited by: M. Hayakawa, Transworld Res. Network, Trivandrum, India, pp.255–279.

Muto, F., Kasahara, Y., Hobara, Y., Hayakawa, M., Rozhnoi, A., Solovieva, M., Molchanov, O.A., 2009, Further study on the role of atmospheric gravity waves on the seismo-ionospheric perturbations as detected by subionospheric VLF/LF propagation, Nat. Haz. Earth Syst. Sci., 9, pp.1111–1118.

Nemec, F., Santolik, O. and Parrot, M., 2009, Decrease of intensity of ELF/VLF waves observed in the upper ionosphere close to earthquakes: A statistical study, J. Geophys. Res., 14, A04303, doi: 10.1029/2008JA013972.

Ouzonov, D., Liu, D. and Kang, C., 2007, Outgoing long wave radiation variability from IR satellite data prior to major earthquakes, Tectonophysics, 431, pp.211–220.

Ouzounov, D., Pulinets, S. and Romanov, A., 2011, Atmosphere-ionosphere response to the M9 Tohoku earthquake revealed by joined satellite and ground observations: Preliminary results, Earthquake Sci., 24, pp.557– 564.

Parrot, M., 1995a, Electromagnetic noise due to earthquakes, in Handbook of Atmospheric Electrodynamics, 2nd ed., edited by: H. Volland, CRC Press, Boca Raton, Fl., 2, pp. 95–116.

Pulinets, S.A., Boyarchuk, K.A., Lomonosov, A.M., Khegai, V.V. and Liu, J.Y., 2002, Ionospheric Precursors to Earthquakes: A Preliminary Analysis of the foF2 Critical Frequencies at Chung-Li Ground-Based Station for Vertical Sounding of the Ionosphere (Taiwan Island), Geomag. and Aeronomy, 42, pp.508–513.

Pulinets, S.A., and Ouzonov, D., 2011, Lithosphere-Atmosphere-Ionosphere Coupling (LAIC) model–An unified concept for earthquake precursors validation, J. Asian Earth Sci., 41, pp.371–381.

Pulinets, S.A., and Boyarchuk, K., 2004, Ionospheric Precursors of Earthquakes, ISBN 3-540-20839-9 Springer, New York.

Ray, S., Chakrabarti, S.K., Sasmal, S. and Choudhury, A.K., 2010, Correlations between the Anomalous Behavior of the Ionosphere and the Seismic Events for VTX-MALDA VLF Propagation, AIP, 1286, pp.298–308.

Ray, S., Chakrabarti, S.K., Mondal, S.K. and Sasmal, S., 2011, Ionospheric anomaly due to seismic activities-III:correlation between night time VLF amplitude fluctuations and effective magnitudes of earthquakes in Indian sub-continent, Nat. Haz. Earth Syst. Sci., 11, pp.2699–2704.

Ray, S., Chakrabarti, S.K., Sasmal, S., 2012, Precursory effects in the nighttime VLF signal amplitude for the 18th January, 2011 Pakistan earthquake, Indian J. Phys., 86(2), pp.85–88.

Ray, S. and Chakrabarti, S.K., 2013, A study on the behavior of the terminator shifts using multiple VLF propagation paths during Pakistan earthquakes (M=7.4), occurred on 19th Jan., 2011, Nat. Haz. Earth Syst. Sci., 13, pp.1501–1506.

Rodger, C.J., Thomson, N.R. and Dowden, R.L., 1996, A search for ELF/VLF activity associated with earthquakes using ISIS satellite data, J. Geophys Res., 101(A6), pp.13369–13378.

Rodger, C.J., Dowden, R.L. and Thomson, N.R., 1999a, Observations of electromagnetic activity associated with earthquakes by low-altitude satellites, in Atmospheric and Ionospheric Electromagnetic Phenomena Associated With Earthquakes, edited by: M. Hayakawa, Terra Sci. Pub. Co., Tokyo, pp.697–710.

Rodger, C.J., Thomson, N.R. and Wait, J.R., 1999b, VLF scattering from red sprites: Vertical columns of ionization in the Earth-ionosphere waveguide, Radio Sci., 34(4), pp.913–921.

Rozhnoi, A., Solovieva, M.S., Molchanov, O.A. and Hayakawa, M., 2004 , Middle latitude LF (40 kHz) phase variations associated with earthquakes for quiet and disturbed geomagnetic conditions, Phys. Chem. Earth, 29 , pp.589–598.

Rozhnoi, A., Molchanov, O.A., Solovieva, M., Gladyshev, V., Akentieva, O., Berthelier, J.J., Parrot, M., Lefeuvre, F., Biagi, P.F., Castellana, L. and Hayakawa, M., 2007a, Possible seismo-ionosphere perturbations revealed by VLF signals collected on ground and on a satellite, Nat. Haz. Earth Syst. Sci., 7, pp.617–624.

Rozhnoi, A., Solovieva, M., Molchanov, O.A., Biagi, P.F. and Hayakawa, M., 2007b, Observation evidences of atmospheric Gravity Waves induced by seismic activity from analysis of subionospheric LF signal spectra, Nat. Haz. Earth Syst. Sci., 7, pp.625–628.

Sasmal, S. and Chakrabarti, S.K., 2009, Ionospheric anomaly due to seismic activities -I: Calibration of the VLF signal of VTX 18.2kHz station from Kolkata, Nat. Haz. Earth Syst. Sci., 9, pp.1403–1408.

Sasmal, S. and Chakrabarti, S.K., 2010, Studies of the Correlation Between Ionospheric Anomalies and Seismic Activities in the Indian Subcontinent, AIP, 1286, pp.270–290.

Sasmal, S., Chakrabarti, S.K. and Ray, S., 2014, Unusual behavior of VLF signals observed from Sitapur during the Earthquake at Honshu, Japan on 11 March, 2011, Indian J. Phys. 88(10), pp.103–1019.

Shalimov, S.L., 1992, Lithosphere-ionosphere relationship: a new way to predict earthquakes? Episodes, International Geophysics Newsmagazine, 15, pp.252–254.

Shvets, A.V., Hayakawa, M., Molchanov, O.A. and Ando, Y., 2004a, A study of ionospheric response to regional seismic activity by VLF radio sounding, Phys. Chem. Earth, 29, pp.627–637.

Shvets, A.V., Hayakawa, M. and Maekawa, S., 2004b, Results of subionospheric radio LF monitoring prior to the Tokachi (m=8,Hokkaido, 25 September 2003) earthquake, Nat. Haz. Earth Syst. Sci., 4, pp.647–653.

Thomson, N. R., 1993, Experimental daytime VLF ionospheric parameters, J. Atmos. Terr. Phys., 55, pp.173–184.

Torrence, C. and Compo, G.P., 1998, A Practical Guide to Wavelet Analysis, Bull. Am. Meteorol. Soc, 79(1), pp.61–78.

Tramutoli, V., Cuomo, V., Filizzola, C., Pergola, N. and Pietrapertosa, C., 2005, Assessing the potential of thermal infrared satellite surveys for monitoring seismically active areas: The case of Kocaeli (Izmit) earthquake, August 17, 1999. Rem. Sens. Environ., 96(3-4), pp.409–426.

Tramutoli, V., Aliano, C., Corrado, R., Filizzola, C., Genzano, N., Lisi, M., Martinelli, G. and Pergola, N., 2013, On the possible origin of Thermal Infrared Radiation (TIR) anomalies in earthquake-prone areas observed using Robust Satellite Techniques (RST), Chem. Geol., 339, pp.157–168.

Trigunait, A., Parrot, M., Pulinets, S. and Li, F., 2004, Variations of the ionospheric electron density during the Bhuj seismic event, Ann. Geophys., 22, pp.4123–4131.

Wait, J.R., 1996, Electromagnetic Waves in Stratified Media, corrected reprinting of 1962 edition, IEEE Press, New York.

Wait, J.R. and Spies, K.P., 1964, Characteristics of the Earth-ionosphere waveguide for VLF radio waves, NBS Tech, Note 300, Nat. Bur. of Stand., Washington, D.C.

Xiong, P., Bi, Y. and Shen, X., 2009a, A Wavelet-based Method for Detecting Seismic Anomalies in Remote Sensing satellite data, Machine Learning and Data Mining in Pattern Recognition, MLDM2009, LNAI5632,
SpringerVerlag Berlin Heidelberg, Berlin, New York, doi: 10.1007/978-3642-030703-43, pp.569–581.

Xiong, P., Bi, Y. and Shen, X., 2009b, Study of Outgoing Longwave Radiation Anomalies Associated with Two Earthquakes in China using Wavelet Maxima, Hybrid Artificial Intelligence Systems, HAIS 2009, LNAI 5572 , Springer-Verlag Berlin Heidelberg, Berlin, New York, doi: 10.1007/9783642-02319-4-10, pp.77–87.

Xiong, P., Shen, X.H., Bi, Y.X., Kang, C.L., Chen, L.Z., Jing, F. and Chen Y., 2010, Study of outgoing longwave radiation anomalies associated with Haiti earthquake, Nat. Haz. Earth Syst. Sci., 10, pp.2169–2178.